2-6-2017

Enzyme–free uric acid electrochemical sensors using β–cyclodextrin modified carboxylic acid functionalized carbon nanotubes

Mulugeta B. Wayu
University of Richmond, mwayu@richmond.edu

Margaret A. Schwarzmann

Samuel D. Gillespie

Michael C. Leopold
University of Richmond, mleopold@richmond.edu

This is a pre-publication author manuscript of the final, published article.

Recommended Citation

M.B. Wayu, M.A. Schwarzmann, S.D. Gillespie, and M.C. Leopold, "Enzyme-free Uric Acid Electrochemical Sensors Using β–cyclodextrin Modified Carboxylic Acid Functionalized Carbon Nanotubes," *Journal of Materials Science* 2017, *52*(10), 6050-6062.

For submission to J. Materials Science

Enzyme–free uric acid electrochemical sensors using β–cyclodextrin modified carboxylic acid functionalized carbon nanotubes

Mulugeta B. Wayu,[†] Margaret A. Schwarzmann,[†] Samuel D. Gillespie, Michael C. Leopold*

Department of Chemistry, Gottwald Center for the Sciences, University of Richmond
Richmond, VA 23173

Abstract

Carboxylic acid functionalized multi–walled carbon nanotubes (COOH–MWCNT) were modified via ultra-sonication with β–cyclodextrin (β–CD) to obtain a COOH–MWCNT:β–CD nanocomposite material for the purpose of developing an enzyme–free electrochemical sensor for uric acid (UA) – a clinically relevant molecule implemented in pregnancy induced hypertension (PIH) diagnosis. The nanocomposite material is deposited onto glassy carbon electrodes, and subsequently capped with layers of Nafion and Hydrothane polyurethane (HPU). The surface morphology and electronic structure of the nanocomposite material were characterized using UV–Vis, TEM and FTIR. The performance of the electrochemical sensor was measured through direct injection of UA during amperometry. With the high surface area of the COOH–MWCNT in concert with the selectivity provided by β–CD, the composite system outperforms similar COOH–MWCNT systems, displaying enhanced UA sensitivity versus films with only COOH–MWCNT. With the improved sensitivity (4.28 ± 0.11 $\mu A \cdot mM^{-1}$), fast response time (4.0 ± 0.5 s), the sensors offer wide detection of UA across clinically relevant ranges (100–700 µM) as well as demonstrated selectivity against various interferents.

[†] These authors contributed equally to this work.

*To whom correspondence should be addressed. Email: mleopold@richmond.edu; Phone: (804) 287-6329; Fax: (804) 287-1897

1. Introduction

Methods for the effective detection of uric acid (2, 6, 8–trihydroxypurine, UA) are gaining a significant attention due to its clinical significance [1–4]. Many diseases such as gout, hyperuricemia, Lesch–Nyhan disease, obesity, diabetes, high cholesterol, high blood pressure, kidney disease and heart disease have been related to the presence of abnormal levels of UA in biological fluids such as blood and urine [5–11]. The presence of high UA levels in the blood of late–term pregnant women can signal a higher probability of pregnancy–induced hypertension (PIH), a condition that leads to a disorder known as pre–eclampsia which places both mothers and babies at significant health risk. Emergency cesarean section surgery, an abdominal surgical intervention, remains a standard procedure to halt PIH progression even in cases where the condition is only suspected based on hypertension assessment. The cost of cesarean section is increasing, costing billions of dollars every year [12]. The ability to reliably measure UA in real–time has been recognized as a viable predictor of PIH that may allow for earlier and more accurate assessment of the condition which, in turn, should decrease the number of unnecessary and costly surgeries [13]. Current UA testing procedures require time–consuming laboratory evaluation of blood/urine [7] during which PIH can remain undiagnosed with increasing probability of serious complications and potential progression toward pre–eclampsia. Thus, effective UA sensors, capable of accurate, fast, and local monitoring at the bedside, are desired in order to detect and predict abnormal conditions [6, 7, 14].

Enzymes have been incorporated at the interface of modified electrodes used as electrochemical sensors in order to increase selectivity of biosensors [1, 14, 15]. The use of enzymes in this capacity, however, invokes indirect measurements of target analyte concentration and are often dependent on the availability of certain enzyme and their kinetics, the latter often resulting in low sensor sensitivity [4]. First generation biosensors, for example, employ enzymatic reactions where an immobilized oxidase enzyme in the presence of oxygen catalyzes a specific analyte and yields the by–product hydrogen peroxide (H_2O_2) which is subsequently oxidized at the working electrode to produce a signal proportional to the analyte concentration [14–17]. While this strategy has been successful for many targets, enzyme–based biosensors have also shown many disadvantages such as poor stability and reproducibility, oxygen dependence, high costs, and lengthy preparation times [2, 18].

Exploring the use of new and novel materials to integrate into sensors for sensitive and selective detection of targeted molecules continues to be an active area of research [19, 20]. Carbon–based nanomaterials gained extensive interest due to their high superficial area, edge–plane–like defect, high conductivity, and chemical inertness [21]. More specifically, carbon nanotubes (CNTs) have been a focus within the electrochemical sensor community [9, 22, 23]. Depending on their atomic structure, CNTs can behave as metallic or semiconductor material and, when incorporated at an electrochemical interface, promote electron–transfer (ET) in chemical reactions [10, 17, 22–26]. Multi–walled carbon nanotubes (MWCNT) are considered to be attractive materials for modifying electrode interfaces due to their large surface areas, high conductivities, and proven electrocatalytic activities, allowing fast ET and reducing over–potentials [27, 28]. However, due to their strong inter–tube van der Waals forces of attraction, the insolubility of CNT in aqueous or organic solvents remains problematic [10] and limits their applications. Numerous methods have been adopted to modify CNT in order to enhance their dispersion in solvents [10, 29]. For instance, *Xing et al.* (2005) sonochemically oxidized MWCNT to increase the population of oxygen containing groups on its surfaces [30]. *Wang et al.* (2003) homogeneously suspended CNT in Nafion–ethanol solutions for the development of selective hydrogen peroxide amperometric biosensor [23]. While dispersion of the CNT within the Nafion matrix is achieved with this strategy, the consequences include decreased effective CNT surface area and lower inter-tube electronic conductivity due to the presence of the Nafion scaffold. Thus, fabrication of an effective electrochemical sensor using CNTs to achieve sensitive, fast and facile detection of UA remains a challenge.

Interest in the use of enzyme–free electrochemical sensors for the detection of UA is increasing [4]. With the use of non–enzymatic, or direct detection of electroactive UA (Eqn.1), the challenge is to introduce effective selectivity without employing an enzymatic reaction [4, 31, 32].

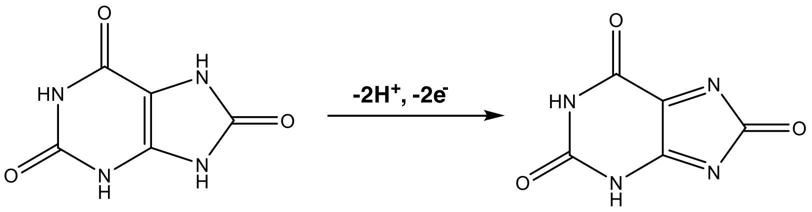

(1)

Cyclodextrins (CD), a naturally occurring macrocyclic glucose oligomers, form doughnut or wreath–shaped truncated cones known as α, β and γ–CD with six, seven and eight D–glucose units, respectively. The α, β and γ–CD structures form molecular cavities of 0.53, 0.65, and 0.83 nm in diameter, respectively [9, 23, 32]. CD comprises a primary and secondary alcohol groups on the smaller and larger edges or rims, respectively. In spite of the hydrophilic rims, CD also exhibits a significantly hydrophobic character in the inner region [33], a product of the C–H bonds that point inwardly toward the cavity. The combination of these functional groups in their molecular structure, enables the CD to form supramolecular complexes with other molecules. For instance, in the cavity structure, hydrophobic molecules can easily be incorporated by displacing the water [26, 33, 34]. More specifically, for example, β–CD can form a host–guest inclusion complex with UA via hydrogen–bonding and hydrophobic interactions [2, 3]. Using this type of complexation, it has been reported that CD immobilized at electrodes provided for enhanced, selective detection of UA in the presence of ascorbic acid, a common interferent species [9, 35-36].

In prior work in our lab, pristine MWCNTs were uniformly dispersed in Nafion-ethanol solution to form a Nafion-MWCNT composite film at the electrode. For selectivity, β–CD was then electropolymerized into the film to create a selective UA sensing platform with effective sensitivity (~ 2 μA/mM) [36]. Even though the report represents a successful proof-of-concept for a UA sensing incorporating MWCNTs, the strategy remains susceptible because the use of Nafion for dispersion likely allows for interference of optimal coupling between the MWCNTs and β–CD, the primary components of the film that provide sensitivity and selectivity, respectively. Thus, exploring CNT dispersion methodology and materials that allow for maintaining MWCNT surface area for maximum interaction of the MWCNTs for maximum coupling interaction with β–CD remains, to our knowledge, a noteworthy and largely unexplored facet of this area of interest.

In the work presented herein, three materials are evaluated in terms of their ability to enhance the performance of an enzyme–free, layer–by–layer (LbL)–constructed UA electrochemical sensor: (1) carboxylic acid functionalized MWCNT (COOH–MWCNT), (2) β–CD adsorbed to the COOH–MWCNT modified electrodes, and (3) outer selective polymer membranes or layers of Nafion and polyurethane (HPU). Most notably, this research focuses on the incorporation of COOH-MWCNT because they are more easily dispersed in aqueous solution compared to pristine

MWCNTs. The increased dispersion in aqueous media allows for the use of ultra-sonication as a method to maximize interaction between COOH–MWCNT and β–CD to form COOH–MWCNT:β–CD composite suspensions and, in theory, produce materials able to selectively detect UA with greater sensitivity than when such material interactions are not optimized [36]. To the best of our knowledge, the effect of sonication as a means of understanding the role of fundamental interactions between the nanomaterials and selective molecules has not yet been explored. Our research includes extensive characterization of the electrode materials using transmission electron microscopy (TEM) and Fourier transform infrared (FTIR) spectroscopy. The electrochemical performance and the electrocatalytic properties of the electrode materials were investigated using cyclic voltammetry (CV) and chronoamperometry (CA). The formative result of this study is the demonstrated construction and performance of an enzyme–free, CNT–based UA sensor with effective sensitivity, selectivity, and stability that suggests potential for continued development toward commercialization.

2. Experimental Section

Materials and Instrumentation

All chemicals were purchased from Sigma–Aldrich, unless stated otherwise. Hydrothane AL25–80A polyurethane (HPU) was obtained from AdvanSource Biomaterials. Nafion (Liquion solution LQ–1105 1100EW 5% wt.) was purchased from Ion Power, Inc. (New Castle, DE, USA). Ultra-pure water (UP H_2O, 18.3 MΩ·cm) was used to prepare all solutions. A Branson 2510 ultra-sonicator (ParaGon Electronics, Pembroke, FL, USA) was used to prepare the electrode materials. An eight–channel potentiostat (CH Instruments, 1000B) was used to record amperometric current–time (I–t) curves to evaluate the performance of the biosensor nanocomposite system. Electrochemical cells were comprised of a common Ag/AgCl (saturated KCl) reference electrode, a common platinum wire counter electrode (Sigma–Aldrich), and modified glassy carbon working electrodes (3 mm diameter, CH Instruments).

Composite Film Fabrication

Glassy Carbon electrodes (GCE) were successively polished with 1.0, 0.3, and 0.05 µm alumina powder, and rinsed thoroughly with UP H_2O. Electrode materials were prepared using ultra-sonication as described elsewhere [37, 38]. Prior to use, the carboxylic acid functionalized multi–walled carbon nanotubes (COOH–MWCNT) were imaged with transmission electron microscopy and deemed typical for this material (Fig. S1).

Sonicated Together. Briefly, in a typical procedure, 2.0 mg of carboxylic acid functionalized multi–walled carbon nanotubes (COOH–MWCNT) and 2.0 mg of cyclodextrin (CD) were added to 1.0 mL of ethanol and dispersed using ultra-sonication to obtain COOH–MWCNT:CD composite suspensions. A 7 µL aliquot of the composite suspension was deposited on newly polished electrodes and allowed to dry for 10 min. The electrodes were subsequently coated with 7 µL aliquots of 0.5% wt. Nafion, and were allowed to dry at room temperature for another 10 min. to obtain GCE/COOH–MWCNT: CD/Nafion.

Sonicated Separately. Similarly, in a typical procedure, 2.0 mg of carboxylic acid functionalized multi–walled carbon nanotubes (COOH–MWCNT) or 2.0 mg of cyclodextrin (CD) was added to 1.0 mL of ethanol and dispersed using ultra-sonication to obtain COOH–MWCNT or CD suspensions respectively. A 7 µL aliquot of each suspension was deposited on newly polished electrodes and allowed to dry for 10 min. The electrodes were subsequently coated with 7 µL aliquots of 0.5% wt. Nafion, and were allowed to dry at room temperature for another 10 min. to obtain GCE/COOH–MWCNT/Nafion, GCE/COOH–MWCNT/CD/Nafion or GCE/CD/Nafion, GCE/CD/COOH–MWCNT/Nafion, respectively.

The outer polyurethane (PU) layer, semipermeable membrane, was applied as previously reported [15, 39–41]. Briefly, 100 mg of Hydrothane polyurethane (HPU) was dissolved in ethanol and THF mixture (1:1) ratio, which was stirred overnight. A 10.0 µL aliquot of the HPU blend was then deposited on the COOH–MWCNT/CD/Nafion modified electrode and allowed to dry (ambient, 30 min.) to obtain GCE/COOH–MWCNT/CD/Nafion/HPU electrochemical sensor. For the purpose of comparison, various electrodes such as GCE/Nafion/HPU, GCE/CD/HPU and GCE/COOH–MWCNT/HPU were prepared in similar fashion.

Evaluation of Sensor Performance

For evaluating the sensors, the various modified electrodes were submerged in 25.0 mL of stirred (1100 rpm) phosphate buffer solution (PBS, 65.55mM, pH 7). The working electrode potential was held at +0.347 V for 1200 seconds prior to consecutive 50 μL injections of 50 mM UA stock solution at 200 second intervals to obtain stair–step response to successive, 100 μM UA increases. Sensor performance was evaluated using linear regression analysis of calibration curves. As in prior work, slopes of calibration curves (i.e., current response vs. UA concentration) corresponded to sensitivity while response times ($t_{R-95\%}$) were defined as the time required to reach 95% of the total change in current due to an increase in UA concentration [40, 41]. Instrumentation details and procedures for transmission electron microscopy (TEM) and Fourier transform infrared (FTIR) spectroscopy and UV–vis spectroscopy characterization of the films is included in Supplementary Information.

3. Results and Discussion

Scheme 1 provides the general, step–by–step design of the enzyme–free layer–by–layer (LbL) UA electrochemical sensor and features four major components modifying a glassy carbon electrode: (1) COOH–MWCNT layer; (2) a layer of adsorbed cyclodextrin, (3) an inner–selective Nafion layer and (4) an outer–selective polyurethane layer. Briefly, as shown, in a typical procedure, COOH–MWCNT is dispersed in ethanol using sonication to form COOH–MWCNT suspension. The COOH–MWCNT suspension is then drop–casted onto freshly polished GCE to obtain GCE/COOH–MWCNT. Then cyclodextrin is coated onto GCE/COOH–MWCNT to obtain GCE/COOH–MWCNT/CD. The ethanol solution of Nafion (0.5% wt.) is then deposited on the as modified electrode to obtain GCE/COOH–MWCNT/CD/Nafion. Finally, HPU is deposited onto GCE/COOH–MWCNT/CD/Nafion and allowed to dry to obtain GCE/COOH–MWCNT/CD/Nafion/HPU. In general, the use of these components in combination was shown to function over extended linear/dynamic ranges of detection with high sensitivity, fast response and selectivity.

3.1. Surface characterization of electrode materials

FTIR spectroscopy was used to initially characterize the materials incorporated into the sensor. **Figure 1** shows characteristic FTIR spectra of the as purchased COOH–MWCNT where a slight signal at ~1720 cm^{-1} is attributed to the presence of the C=O functional group. The weakness of this peak for the as–received COOH–MWCNT suggests that there are low concentrations of carboxylic acid functional groups, likely localized to the edges of the tubes [42]. The spectra of the as–received β–CD is as expected as well, matching the literature [29] with strong absorption bands for –OH and C=O stretches at ~3300 and ~1720 cm^{-1}, respectively. In a typical procedure for sensor construction, the COOH–MWCNT are modified with β–CD via sonication, either separately or together. When the COOH–MWCNT are exposed to β–CD in this manner, the FTIR of the resulting material (Figure 1) maintains signature stretches of β–CD. A representative FTIR spectra of the resulting material prepared in this manner is shown in Figure 1. Peaks observed at 3300, 2930 and 1020 cm^{-1} in β–CD/COOH–MWCNT spectra corresponded to the bending vibration of –OH group, stretching vibrations of $–CH_2–$ and –C–O–C– groups of β–CD, respectively [29]. To help affirm that β–CD exists within the material as a complex with COOH–MWCNT, the material was extensively washed with ethanol to remove excess β–CD. The resulting spectrum of that material (Figure 1) shows the same persistent absorption bands consistent with the β–CD signature.

For additional base–line characterization of the materials, UV–Vis spectroscopy was used to evaluate the efficiency of COOH–MWCNT dispersion in ethanol. Serial dilutions of the COOH–MWCNT suspensions were made and UV–Vis spectra were collected (Fig. S2). The absorbance peak at 230 nm increases with the COOH–MWCNT suspension concentration, consistent with literature reports [43]. The absorption intensity is notably proportional with COOH–MWCNT concentration, underscoring the dispersibility of COOH–MWCNT in ethanol without the help of surfactants. As observed from this assessment (Fig. S2a), ~2 mg/mL of COOH–MWCNT concentration is used as a standard in this study.

Electrodes were modified with COOH–MWCNT sonicated separately or in combination with β–CD in ethanol and subsequently covered with an outer selective layer of Nafion for the direct electrochemical detection of UA. The outer selective layer of Nafion has been shown to be selective for UA [44]. Since UA is electroactive, cyclic voltammetry of 1 mM UA in PBS (pH = 7.0) at various modified electrodes, including bare, COOH–MWCNT modified GCE and COOH–MWCNT:β–CD modified GCE, each coated with Nafion showed the presence of a strong UA oxidation peaks at +0.347 V with both peak shape and potential consistent with prior work [14]. Representative examples of the observed CV are included in Supplementary Information (Fig. S3) and also illustrate the notable increase in background charging current from systems incorporated with COOH–MWCNT and their increased surface area. Based on the peak potential of this UA oxidation, electrodes to be tested as UA sensors were held at +0.347 V vs Ag/AgCl during chronoamperometry to generate current–time (I–t) curves during the standardized injections of UA.

3.2. Optimization of LbL UA Electrochemical Sensor

Common to LbL construction of modified electrodes, initial attempts to utilize these materials consisted of drop–casting the material directly onto the electrodes. The amperometric I–t curves during UA injections and their corresponding calibration curves are shown in **Figure 2**. Systems without nanomaterials, GCE/Nafion/HPU and GCE/β–CD/Nafion/HPU, showed similar and very poor sensitivity (0.02 ± 0.004 $\mu A \cdot mM^{-1}$) toward UA (Figs. 2a, 2b). The same systems with COOH–MWCNT incorporated showed significantly enhanced UA sensitivity. GCE/COOH–MWCNT/Nafion/HPU, for example, exhibited a drastically improved sensitivity of 0.33 ± 0.093 $\mu A \cdot mM^{-1}$ (Fig. 2c). However, when COOH–MWCNT is mixed with β–CD and used to modify GCE to form GCE/COOH–MWCNT:β–CD/Nafion/HPU, the sensitivity increased to 1.23 ± 0.20 $\mu A \cdot mM^{-1}$ (Fig. 2d), indicating the potential synergistic effect of these materials and suggesting a more effective engagement of the selectivity provided by the β–CD. A similar effect is observed when the same layering of materials is executed without the HPU capping layer (Supporting Material, Fig. S4).

With a preliminary result suggesting that the critical component of the sensing scheme may be optimizing the interaction between β–CD and the COOH–MWCNT, the different materials were sonicated either together (i.e., combined) or separately prior to incorporation in the LbL construction of the UA electrochemical sensors. Sonication was employed with the thought that it would further disperse the COOH–MWCNT and provide a greater total surface area of the material to interact with the β–CD. As such, mixtures of COOH–MWCNT and β–CD (1:1) were sonicated for different amounts of time (5 to 60 minutes) to see if there were differences in the COOH–MWCNT:β–CD nanocomposite formation. At various time intervals, nanocomposite material was extracted from the mixture and deposited onto electrodes before being capped with the polymer layers (i.e., Nafion and HPU) and subsequently tested for UA responsiveness. **Figure 3A** shows the effect of sonication time on performance of the systems in terms of amperometric I–t response and corresponding calibration curve (Fig. 3A, inset). As seen in the figure, sensor performance, in terms of sensitivity, is significantly affected by sonication time, increasing from 5 to 45 min. before decreasing gradually at higher sonication times (**Figure 3B).** While a 4–fold increase in sensitivity was observed for 45-minute sonication compared to the 5-minute sonication, the linear range of the calibration curve for the material sonicated at 45 minutes was also affected, limited to 0.4 mM and insufficient for the complete physiological range of UA (0.2 to 0.5 mM UA) [1]. As a result, 30 min. sonication times, which yielded moderate sensitivity over the wider linear range of detection, was selected as optimal for this study.

In optimizing the performance of the electrochemical sensor, other parameters that may affect the electrochemical sensor activity were identified as well, including the ratio of COOH–MWCNT to β–CD in the nanocomposite mixtures, the type or size of the CD molecules, and if sonicating the materials separately or as a mixture. In the first case, the effect of varying the ratio of COOH–MWCNT to β–CD was displayed in Fig. S5. While slightly higher sensitivity was observed when a 1:1 ratio of COOH–MWCNT to β–CD was used to fabricate the sensor, the difference in enhancement compared to the 1:3 and 3:1 ratio was relatively statistically insignificant. Secondly, to confirm that the β–CD is providing enhancement by sequestering UA into its specific size cavities, a series of COOH–MWCNT modified electrodes was investigated incorporating α (smaller cavity), β and γ (larger cavity) CD structures. A 1:1 ratio of COOH–MWCNT to various CD types (i.e.; α, β and γ respectively) were sonicated in ethanol prior to electrode modification as previously described. The current response obtained from I–t curves during the successive injections of UA was translated to the calibration curves (Supplementary Information, Fig. S6) and their slopes (i.e., sensitivities) compared. The greatest sensitivity was achieved using β–CD, ~2.8X and ~1.2X greater than α and γ–CD, respectively. These results imply that the size of the β–CD cavity is indeed playing a role in the selective detection of UA with these systems.

The effect of sequential layering of individual materials, as opposed to applying a single layer mixture of β–CD and COOH-MWCNT, at the electrode was investigated to assess the effect of each material on the electrochemical detection of UA. **Figure 4A** displays the typical I-t curves and the corresponding calibration curves of electrochemical sensors fabricated by applying as received and untreated (i.e., not sonicated) materials as individual layers at the electrode. Here, electrodes with COOH-MWCNT applied at immediate interface and covered with a second layer of β–CD material are compared to similar electrodes with the materials deposited sequentially and in opposite order – both capped with Nafion and HPU. The results show a significant variation in sensitivity when the bottom layer is COOH-MWCNT (Fig. 4A, b) versus the same materials with the bottom layer deposited as β–CD (Fig. 4A, a). The observed results suggest that electronic coupling of the electrode to the COOH-MWCNT material is a critical component toward effectively incorporating the nanotubes into the sensing mechanism, likely extending the effective surface area of the electrode and providing increased interactions with β–CD over that area. The critical nature of the order of layering materials is an established phenomenon in many LbL constructs of sensors and biosensors [14, 41].

Given the success of sonicating the mixture of materials (Fig. 3), a set of experiments focused on the order of layering materials that were individually treated with sonication were conducted. In this case, all materials were sonicated prior to being incorporating into the LbL electrochemical system as individual layers – again testing if enhanced signals were more substantial if sonicated COOH-MWCNT are layered first. **Figure 4B** shows the typical I-t curves and the corresponding calibration curves of electrochemical sensors fabricated using materials that are separately sonicated, denoted with * in the results. Consistent with the trend of Fig. 4A, systems with COOH-MWCNT layered as the first component at the electrode followed by β–CD (and capped with Nafion and HPU) significantly outperformed analogous systems where sonicated β–CD was deposited as the initial layer. Experiments were also conducted where only one component was sonicated as well and resulted in establishing that sonication was beneficial for both β–CD and COOH-MWCNT but that the layering of COOH-MWCNTs as an initial layer was a more dominant factor in improving sensitivity (Supplementary Information, Fig. S7).

Sonicating and depositing both COOH-MWCNT and β–CD individually in conjunction with specifically layering the materials with COOH-MWCNT at the electrode interface produced a superior result. The enhancement from this synergistic effect and the clear benefit of sonication are illustrated in the comparison of results shown in **Figure 4C**. Systems utilizing mixtures of COOH-MWCNT and β–CD were compared with and without sonication prior to deposition and showed significant enhancement of sensitivity with the sonication, increasing from 0.57 ± 0.02 μA·mM^{-1} (Fig. 4C, a) to 3.03 ± 0.15 μA·mM^{-1} (Fig. 4C, c). Layering individual components sequentially, with COOH-MWCNT as the initial layer, showed a similar effect with sonicating the materials, with sensitivity increasing from 0.99 ± 0.01 μA·mM^{-1} (Fig. 4C, b) to 4.28 ± 0.11 μA·mM^{-1} (Fig. 4C, d). This full system, GCE/COOH-MWCNT*/β–CD*/Nafion/HPU, consistently yielded the highest sensitivity of the entire study. We believe the observed enhancement can be attributed to a number of factors. Sonication of the COOH-MWCNT prior to being deposited as the initial layer allows for greater dispersion of the material which then increases the available conductive surface area and maximizes the material's ability to interact with β–CD. The improved interaction likely increases electron transfer properties of the interface with UA[9]. Sonication of the β–CD likely improves the solubility of the material with also serves to optimize its interaction with the COOH-MWCNT. The reasoning behind the relatively less impressive performance of the sonicated mixture of materials is not entirely clear. It may be that the presence of the β–CD with the COOH-MWCNT during sonication may alter the ability of the latter material to disperse as efficiently. Given the results, the optimized system, GCE/COOH-MWCNT*/β–CD*/Nafion/HPU was evaluated for sensor performance.

3.3. LbL UA Electrochemical Sensor Performance

Composite LbL films featuring the separately sonicated layers of COOH–MWCNT and β–CD exhibit high sensitivity (4.28 ± 0.11 μA·mM^{-1}), fast response time (~ 4–5 s), and dynamic/linear ranges (0.1 to 0.7 mM) that easily span physiologically relevant concentrations of UA. As part of evaluating the selectivity of the system, the influences of possible interfering species on the detection of UA was also investigated. The assessment of the selectivity of GCE/COOH–MWCNT*/β–CD*/Nafion/HPU electrochemical sensor is shown in **Figure 5** where the complete film is subjected to injections of common interferents as well as UA injections of different concentrations with the electrode poised at +0.347V. Injections of most interfering species (e.g., sodium nitrite, oxalic acid (OA), and glucose) did not result in significant current response relative to the observed UA response. Ascorbic acid (AA) gave a lower response compared to that of UA. As in prior reports, the most problematic interferent for UA sensing remains acetaminophen (AP). While this represents a challenge, it is important to remember that acetaminophen is a synthetic pharmaceutical that is ingested and clears the body in a relatively short time (4–6 hours). In any eventual medical application of these sensors, the presence of acetaminophen will be identifiable by recording an effective patient history [14, 45].

As has been done in previous studies [15, 39–41] for a quantitative and conservative evaluation of selectivity, the I–t curve responses toward interferents versus the UA analyte can be used to calculate selectivity coefficients (K^{amp}) according to the following equation:

$$K_j^{amp} = \log\left(\frac{\Delta I_j/C_j}{\Delta I_{UA}/C_{UA}}\right) \tag{2}$$

where ΔI_j and ΔI_{UA} are the measured currents for a specific interferent species (j) and uric acid and C_j and C_{UA} are concentrations of the interferent species and UA, respectively. Negative selectivity coefficients indicate that the interferent is inconsequential whereas species with positive values are selected for by the sensor, in this case, only acetaminophen (AP) and UA. Figure 5 (inset), displays a graphical comparison of selectivity coefficients for the GCE/COOH–MWCNT/β–CD/Nafion/HPU electrochemical sensor at +0.347 V. Figure 5 underscores the critical selectivity of the sensor with selectivity coefficients of 0.37 and 0.25 for UA and AA, respectively. Negative selectivity coefficients were observed for sodium nitrite, OA, and glucose. Except for AP, selectivity coefficient values for this UA electrochemical sensing are in agreement with selectivity deemed effective for other reported biosensing schemes [39]. As with many other UA sensors [1], AP, with a selectivity coefficient of 0.69 at +0.347 V, remains a problematic species during sensing, although its selectivity coefficient reported here is lower than that reported in literature for other sensors where AP is considered as an interferent [40, 41, 46].

As previously stated, the electrochemical sensor exhibits excellent response time ($t_{R-95\%}$) of ~ 4 – 5 seconds, a conservative estimate of the response where the time is measured once 95% of the total current change is achieved [40, 41]. Both the sensitivity and response time are generally stable for at least 12 days (**Figure 5**), indicating the potential application of the developed sensor for monitoring of near-term pregnant women with PIH. Additionally, the current response for a single UA concentration at the center of the relevant physiological range (300 μM) was specifically tracked for a set of composite films over the course of 12 days as well (Supplementary Information, Fig. S8) and resulted in an average current response of 0.34 μA/day with a standard deviation of ±0.03 μA/day - an additional indicator of sensor stability. A complete table summary of the performance of the complete system (GCE/COOH–MWCNT*/β–CD*/Nafion/HPU) and comparison of these properties to other related literature reports of uric acid sensors is provided in the Supplementary Information (Table SI–1).

4. Conclusion

In this study, MWCNT-β–CD composite films have been incorporated into LbL constructed electrochemical UA sensors and provided a system that delivers a greater understanding of the critical interaction between the materials used to provide sensitivity and selectivity. The use of ultra-sonication to disperse COOH MWCNTs and maximize interaction with UA selective β-CD created composite films capable of high UA loading capacity coupled with effective electronic communication. By focusing on methodology and materials that optimize the coupling of the advantageous properties of these materials, the sensitivity of the sensor produced was double that of strategies utilizing the same materials without such an emphasis [36]. The developed electrochemical sensor also demonstrated effective selectivity and high reproducibility for the stable detection of UA over time, underscoring the potential of its application for analysis of real samples. One of the advantages of the electrocatalytic activity provided by the incorporation of MWCNT is that the sensor can operate at lower potentials. The sensor presented using an applied potential of +0.347V versus many traditional sensors that use higher voltages. A prime example of such sensors is the widely explored 1st generation schemes that detect hydrogen peroxide oxidation at +0.65 V as it is a by–product of an enzymatic reaction that indirectly signals the presence of an analyte [14, 45, 46]. The present work offers a new avenue to broaden the analytical applications of carbon nanotubes hybrids in clinical analysis.

Acknowledgments

This research was generously supported by funding from the National Science Foundation (CHE–1401593), Commonwealth Health Research Board, the College of Arts and Sciences (MAS), and the Department of Chemistry's Puryear–Topham–Pierce Endowment (SDG). We would like to specifically thank Microscopy Director Christine A. Lacy (TEM and SEM) for her important contributions to this work. We gratefully acknowledge the following people for making research possible at the University of Richmond: Drs. T. Leopold, R. Kanters, D. Kellogg, R. Miller, and R. Coppage, as well as Russ Collins, Phil Joseph, Mandy Mallory, and Lamont Cheatham.

References

[1] Erden PE, Kılıç E (2013) A review of enzymatic uric acid biosensors based on amperometric detection. Talanta 107:312–23.

[2] Li Y, Zhai X, Wang H, Liu X, Guo L, Ji X, Wang L, Qiu H, Liu X (2015) Non–enzymatic sensing of uric acid using a carbon nanotube ionic–liquid paste electrode modified with poly(β–cyclodextrin). Microchim. Acta 182:1877–84.

[3] Wu S, Wang T, Gao Z, Xu H, Zhou B, Wang C (2008) Selective detection of uric acid in the presence of ascorbic acid at physiological pH by using a β–cyclodextrin modified copolymer of sulfanilic acid and N–acetylaniline. Biosens. Bioelectron. 23:1776–80.

[4] Chen X, Wu G, Cai Z, Oyama M, Chen X (2014) Advances in enzyme–free electrochemical sensors for hydrogen peroxide, glucose, and uric acid. Microchim. Acta 181:689–705.

[5] Chauhan N, Pundir CS (2011) An amperometric uric acid biosensor based on multiwalled carbon nanotube–gold nanoparticle composite. Anal. Biochem. 413:97–103.

[6] Retna Raj C, Ohsaka T (2003) Voltammetric detection of uric acid in the presence of ascorbic acid at a gold electrode modified with a self–assembled monolayer of heteroaromatic thiol. J. Electroanal. Chem. 540:69–77.

[7] Lakshmi D, Whitcombe MJ, Davis F, Sharma PS, Prasad BB (2011) Electrochemical Detection of Uric Acid in Mixed and Clinical Samples: A Review. Electroanal. 23:305–20.

[8] Moraes ML, Rodrigues Filho UP, Oliveira ON, Ferreira M (2007) Immobilization of uricase in layer–by–layer films used in amperometric biosensors for uric acid. J. Solid State Electrochem. 11:1489–95.

[9] Wang Z, Wang Y, Luo G (2002) A selective voltammetric method for uric acid detection at [small beta]–cyclodextrin modified electrode incorporating carbon nanotubes. Analyst 127:1353–8.

[10] Erden PE, Kaçar C, Öztürk F, Kılıç E (2015) Amperometric uric acid biosensor based on poly(vinylferrocene)–gelatin–carboxylated multiwalled carbon nanotube modified glassy carbon electrode. Talanta 134:488–95.

[11] Li Y, Ran G, Yi WJ, Luo HQ, Li NB (2012) A glassy carbon electrode modified with graphene and poly(acridine red) for sensing uric acid. Microchim. Acta 178:115–21.

[12] Stafford RS (1990) Cesarean section use and source of payment: an analysis of California hospital discharge abstracts. Am. J. Public Health 80:313–5.

[13] Roberts JM, Bodnar LM, Lain KY, Hubel CA, Markovic N, Ness RB, Powers RW (2005) Uric acid is as important as proteinuria in identifying fetal risk in women with gestational hypertension. Hypertension 46:1263–9.

[14] Conway GE, Lambertson RH, Schwarzmann MA, Pannell MJ, Kerins HW, Rubenstein KJ, Dattelbaum JD, Leopold MC (2016) Layer–by–layer design and optimization of xerogel–based amperometric first generation biosensors for uric acid. J. Electroanal. Chem. 775:135–45.

[15] Poulos NG, Hall JR, Leopold MC (2015) Functional Layer–By–Layer Design of Xerogel–Based First–Generation Amperometric Glucose Biosensors. Langmuir 31:1547–55.

[16] DiPasquale LT, Poulos NG, Hall JR, Minocha A, Bui TA, Leopold MC (2015) Structure–function relationships affecting the sensing mechanism of monolayer–protected cluster doped xerogel amperometric glucose biosensors. J. Colloid Interface Sci. 450:202–12.

[17] Wang J. (2005) Carbon–nanotube based electrochemical biosensors: a review. Electroanal. 17:7–14.

[18] Alarcón–Ángeles G, Guix M, Silva WC, Ramírez–Silva MT, Palomar–Pardavé M, Romero–Romo M, Merkoçi A (2010) Enzyme entrapment by β–cyclodextrin electropolymerization onto a carbon nanotubes–modified screen–printed electrode. Biosens. Bioelectron. 26:1768–73.

[19] Wang Z, Dong X, Li J (2008) An inlaying ultra–thin carbon paste electrode modified with functional single–wall carbon nanotubes for simultaneous determination of three purine derivatives. Sens. Actuators B: Chem. 131:411–6.

[20] Bello A, Giannetto M, Mori G, Seeber R, Terzi F, Zanardi C (2007) Optimization of the DPV potential waveform for determination of ascorbic acid on PEDOT–modified electrodes. Sens. Actuators B: Chem. 121:430–5.

[21] Du J, Yue R, Yao Z, Jiang F, Du Y, Yang P, Wang, C (2013) Nonenzymatic uric acid electrochemical sensor based on graphene–modified carbon fiber electrode. Colloids Surf. A Physicochem. Eng. Asp. 419:94–9.

[22] Wayu MB, King JE, Johnson JA, Chusuei CC (2015) A Zinc Oxide Carbon Nanotube Based Sensor for In Situ Monitoring of Hydrogen Peroxide in Swimming Pools. Electroanal. 27:2552–8.

[23] Wang J, Musameh M, Lin Y (2003) Solubilization of Carbon Nanotubes by Nafion toward the Preparation of Amperometric Biosensors. J. ACS 125:2408–9.

[24] Shi J, Claussen JC, McLamore ES, ul Haque A, Jaroch D, Diggs AR, Calvo-Marzal, P. Rickus, JL Porterfield, DM (2011) A comparative study of enzyme immobilization strategies for multi–walled carbon nanotube glucose biosensors. Nanotechnol. 22: 355502

[25] Gooding JJ (2005) Nanostructuring electrodes with carbon nanotubes: A review on electrochemistry and applications for sensing. Electrochim. Acta 50:3049–60.

[26] Yang H, Zhu Y, Chen D, Li C, Chen S, Ge Z (2010) Electrochemical biosensing platforms using poly–cyclodextrin and carbon nanotube composite. Biosens. Bioelectron. 26:295–8.

[27] Li J, Feng H, Feng Y, Liu J, Liu Y, Jiang J, Qian D (2014) A glassy carbon electrode modified with β–cyclodextin, multiwalled carbon nanotubes and graphene oxide for sensitive determination of 1,3–dinitrobenzene. Microchim. Acta 181:1369–77.

[28] Gao Y–S, Wu L–P, Zhang K–X, Xu J–K, Lu L–M, Zhu X–F, Wu Y (2015) Electroanalytical method for determination of shikonin based on the enhancement effect of cyclodextrin functionalized carbon nanotubes. Chin. Chem. Lett. 26:613–8.

[29] He Y, Xu Z, Yang Q, Wu F, Liang L (2015) Supramolecular modification of multi–walled carbon nanotubes with β–cyclodextrin for better dispersibility. J. Nanopart. Res. 17:1–10.

[30] Xing Y, Li L, Chusuei CC, Hull RV (2005) Sonochemical Oxidation of Multiwalled Carbon Nanotubes. Langmuir 21:4185–90.

[31] Tian L, Zhang B, Sun D, Chen R, Wang B, Li T (2014) A thin poly(acridine orange) film containing reduced graphene oxide for voltammetric simultaneous sensing of ascorbic acid and uric acid. Microchim. Acta 181:589–95.

[32] Rafati AA, Afraz A, Hajian A, Assari P (2014) Simultaneous determination of ascorbic acid, dopamine, and uric acid using a carbon paste electrode modified with multiwalled carbon nanotubes, ionic liquid, and palladium nanoparticles. Microchim. Acta 181:1999–2008.

[33] Szejtli J (1998) Introduction and General Overview of Cyclodextrin Chemistry. Chem. Rev. 98:1743–54.

[34] Soylemez S, Hacioglu SO, Kesik M, Unay H, Cirpan A, Toppare L (2014) A Novel and Effective Surface Design: Conducting Polymer/beta–Cyclodextrin Host–Guest System for Cholesterol Biosensor. Acs Appl. Mater. Interfaces 6:18290–300.

[35] Zheng L, Wu S, Lin X, Nie L, Rui L (2001) Selective Determination of Uric Acid by Using a β–Cyclodextrin Modified Electrode. Electroanalysis 13:1351–4.

[36] Wayu MB, DiPasquale LT, Schwarzmann MA, Gillespie SD, Leopold MC (2016) Electropolymerization of β-cyclodextrin onto multi-walled carbon nanotube composite films for enhanced selective detection of uric acid. J. Electroanal. Chem. 783:192-200.

[37] Fang B, Zhang C, Zhang W, Wang G (2009) A novel hydrazine electrochemical sensor based on a carbon nanotube–wired ZnO nanoflower–modified electrode. Electrochim. Acta 55:178–82.

[38] Wayu MB, Spidle RT, Devkota T, Deb AK, Delong RK, Ghosh KC, Wanekaya, AK. Chusuei, CC (2013) Morphology of hydrothermally synthesized ZnO nanoparticles tethered to carbon nanotubes affects electrocatalytic activity for H_2O_2 detection. Electrochim. Acta 97:99–104.

[39] Koh A, Lu Y, Schoenfisch MH (2013) Fabrication of Nitric Oxide–Releasing Porous Polyurethane Membranes–Coated Needle–type Implantable Glucose Biosensors. Anal. Chem. 85:10488–94.

[40] Freeman MH, Hall JR, Leopold MC (2013) Monolayer–Protected Nanoparticle Doped Xerogels as Functional Components of Amperometric Glucose Biosensors. Anal. Chem. 85:4057–65.

[41] Wayu MB, Pannell MJ, Leopold MC (2016) Layered Xerogel Films Incorporating Monolayer–Protected Cluster Networks on Platinum–Black–Modified Electrodes for Enhanced Sensitivity in First–Generation Uric Acid Biosensing. ChemElectroChem 3:1245-1252.

[42] Kim C, Seo K, Kim B, Park N, Choi YS, Park KA, Lee, YH (2003) Tip–functionalized carbon nanotubes under electric fields. Phys. Rev. B 68:115403.

[43] Fei T, Jiang K, Jiang F, Mu R, Zhang T (2014) Humidity switching properties of sensors based on multiwalled carbon nanotubes/polyvinyl alcohol composite films. J. Appl. Polym. Sci. 131:39726.

[44] Cao X, Luo L, Ding Y, Yu D, Gao Y (2009) Simultaneous determination of dopamine and uric acid on nafion/sodium dodecylbenzenesulfonate composite film modified glassy carbon electrode. J. Appl. Electrochem. 39:1603–8.

[45] Chen K, Conway GE, Hamilton GA, Trawick ML, Leopold MC (2016) Electropolymerized layers as selective membranes in first generation uric acid biosensors. J. Appl. Electrochem. 1–13.

[46] Koh A, Riccio DA, Sun B, Carpenter AW, Nichols SP, Schoenfisch MH (2011) Fabrication of nitric oxide–releasing polyurethane glucose sensor membranes. Biosens. Bioelectron. 28:17–24.